PAPER

Check for updates

The quercetin metabolite 4-methylcatechol causes vasodilation *via* voltage-gated potassium (K_V) channels†

Patrícia Dias,‡[a,b] Rudy Salam, [iD] ‡[c,d] Jana Pourová, [iD] [a] Marie Vopršalová,[a] Lukáš Konečný,[a] Eduard Jirkovský, [iD] [a] Jurjen Duintjer Tebbens [iD] [c] and Přemysl Mladěnka [iD] *[a]

Dietary polyphenols have been associated with many beneficial cardiovascular effects. However, these effects are rather attributed to small phenolic metabolites formed by the gut microbiota, which reach sufficient concentrations in systemic circulation. 4-Methylcatechol (4-MC) is one such metabolite. As it is shown to possess considerable vasorelaxant effects, this study aimed to unravel its mechanism of action. To this end, experimental *in vitro* and *in silico* approaches were employed. In the first step, isometric tension recordings were performed on rat aortic rings. 4-MC potentiated the effect of cyclic nucleotides, but the effect was not mediated by either soluble guanylyl cyclase (sGC), modification of cyclic adenosine monophosphate levels, or protein kinase G. Hence, downstream targets such as calcium or potassium channels were considered. Inhibition of voltage-gated K$^+$ channels (K$_V$) markedly decreased the effect of 4-MC, and vasodilation was partly decreased by inhibition of the K$_V$7 isoform. Contrarily, other types of K$^+$ channels or L-type Ca^{2+} channels were not involved. *In silico* reverse docking confirmed that 4-MC binds to K$_V$7.4 through hydrogen bonding and hydrophobic interactions. In particular, it interacts with two crucial residues for K$_V$7.4 activation: Trp242 and Phe246. In summary, our findings suggested that 4-MC exerts vasorelaxation by opening K$_V$ channels with the involvement of K$_V$7.4.

Introduction

Hypertension is a multifactorial and, in its early stages, a silent disease that affects more than 30% of the adult population worldwide. It can cause or facilitate a cardiovascular event and even premature death.[1] Arterial blood pressure is basically determined by two parameters: cardiac output and total peripheral resistance. In many cases, hypertensive patients have an unaltered cardiac output, whereas the total peripheral resistance is elevated.[2] This fact highlights the major role played by blood vessels in the pathogenesis of hypertension. Indeed, small arteries and arterioles often appear more constricted and thicker in hypertension owing to abnormalities in vascular smooth muscle cells (VSMCs).[3] Physiologically, the dynamic changes in vessel contractility are monitored by a tight interplay between the potassium (K$^+$) and calcium (Ca^{2+}) channels located in VSMCs. However, in chronic hypertension, vascular remodeling frequently occurs and contributes to an abnormal depolarized state of VSMCs.[2,4] Flavonoids are polyphenolic substances that are abundant in foods such as vegetables, fruits, tea, red wine, and dark chocolate and have been positively linked to protective effects on the cardiovascular system.[5,6] Indeed, epidemiological studies have suggested that a high intake of flavonoids is inversely related to arterial blood pressure.[7] The probable explanation for this phenomenon is based on vasorelaxation as a consequence of flavonoid intake. However, flavonoids are not active *in vivo* in their parent forms as they are poorly absorbed.[8] Hence, rather their metabolites, most commonly small phenolic compounds formed by human microflora, are responsible for such an effect. To date, a large repertoire of small phenolic metabolites has been identified and detected in human biological fluids[9–11] and many have been shown to relax in different magnitude vessels *in vitro* or even *in vivo*.[12–15] Yet, in most cases, the mechanisms of action of these metabolites remain enigmatic as there has not been much research in this field.

[a]*Department of Pharmacology and Toxicology, Faculty of Pharmacy, Charles University, Hradec Kralove, 500 05, Czech Republic. E-mail: mladenkap@faf.cuni.cz; Fax: +420 495 067 170; Tel: +420 495 067 295*
[b]*Division of Outcomes & Translational Sciences, Pelotonia Research Center, The Ohio State University, 2255 Kenny Rd, Columbus, OH, USA*
[c]*Department of Biophysics and Physical Chemistry, Faculty of Pharmacy, Charles University, Hradec Kralove, 500 05, Czech Republic*
[d]*Department of Pharmacy, Faculty of Medicine, Brawijaya University, Malang, Indonesia*
†Electronic supplementary information (ESI) available. See DOI: https://doi.org/10.1039/d3fo04672a
‡These authors have contributed equally to this work.

4-Methylcatechol (4-MC) is one such metabolite. It was suggested to be formed upon microbial catabolism of different classes of (poly)phenols (*e.g.*, flavonol, quercetin, and its glycosides, flavan-3-ols, chlorogenic acids, Fig. 1).[9,16] Although its detection in the urine of rats fed with vanillin was described as early as in the mid-1970s,[17] its significant vasorelaxant effects were discovered by our team recently, and such data were confirmed in animals where 4-MC was able to decrease arterial blood pressure.[14,15] More concretely, 4-MC induced relaxation of the rat aorta and mesenteric arteries *in vitro*, and caused a drop in the mean arterial pressure by 10% in spontaneously hypertensive rats after a single i.v. dose of 2.5 mg kg^{-1}. Importantly, the observed effects were not mediated through the heart, and most likely relied on a decrease in the resistance of the vasculature.[14] Therefore, the aim of the current study was to unravel the specific mechanisms that mediate the vasodilatory action of 4-MC. To achieve this, we carried out *in vitro* experiments on the isolated rat aorta, and *in silico* reverse docking studies.

Materials and methods

Animals

For the *in vitro* experiments, male Wistar Han rats (*n* = 32) obtained from Charles River, Germany (av. weight 300 g) were

Fig. 1 Simplified scheme of the suggested metabolic pathways for distinct classes of polyphenols leading to the formation of 4-methylcatechol: (a) procyanidin (PC), (b) chlorogenic acids, (c) flavonol rutin, and (d) vanillin. Data were obtained from the following ref. 9 and 17–22.

used. The animals were bred in the animal facility of the Faculty of Pharmacy, Charles University, and maintained at a constant temperature of 23–25 °C with the 12 h dark/light cycle. Rats were provided a standard diet and tap water *ad libitum*. The study was conformed to The Guide for the Care and Use of Laboratory Animals published by the US National Institutes of Health (8th edition, revised 2011, ISBN-13:978-0-309-15400-0), and was performed in agreement with approval of the Czech Ministry of Education, Youth and Sports (No. 4937_2019-9).

Chemicals

Urethane, noradrenaline, acetylcholine, sodium nitroprusside (SNP), dimethyl sulfoxide (DMSO), nifedipine, 1*H*-[1,2,4]oxadiazolo[4,3-*a*]quinoxalin-1-one (ODQ), membrane-permeable protein kinase G Iα inhibitory peptide: RQIKIWFQNRRMKWKKLRKKKKKH (DT-3), forskolin, bradykinin, iberiotoxin, glibenclamide, BaCl$_2$, 4-aminopyridine, linopirdine, and thapsigargin, as well as the tested compound 4-MC were purchased from Sigma-Aldrich (Germany). Bay K8644 was obtained from Axon Medchem BV (Netherlands). 4-MC was dissolved in 100% DMSO (10 mM), and the subsequent solutions were prepared with ultrapure water. KCl and CaCl$_2$ were purchased from Sigma-Aldrich. NaCl, NaHCO$_3$, and D-glucose were provided by PENTA s.r.o. (Czech Republic), MgSO$_4$·7H$_2$O was purchased from Erba Lachema (Czech Republic) s.r.o., whereas KH$_2$PO$_4$ was obtained from Dr Kulich Pharma s.r.o. (Czech Republic). The Krebs solution contained the following composition in mM: NaCl, 119; KCl, 4.7; CaCl$_2$, 1.25; KH$_2$PO$_4$, 1.18; MgSO$_4$·7H$_2$O, 1.17; NaHCO$_3$, 25; and D-glucose, 11.

In vitro experiments

Rat aorta isolation. Rats were anaesthetized by administration of urethane (1.2 g kg^{-1}, intraperitoneally) and sacrificed by exsanguination. The thoracic aorta was excised, immersed in the Krebs solution, and cleaned of adherent fat, connective tissue, and blood, and cut into 3 mm long rings. In certain experiments, the endothelial layer of the aortic rings was mechanically disrupted by gently rubbing the luminal surface with dental floss. The rings were maintained in tissue baths filled with the Krebs solution aerated with 5% CO$_2$ in O$_2$, at 37 °C. Each aortic ring was hung between two stainless-steel wire hooks, one fixed to a holder and the second connected to a transducer and computer equipped with SPEL Advanced Kymograph Software, v3.2 (Experimetria Ltd, Hungary). This arrangement enabled the measurement of isometric tensions. Subsequently, the aortic rings were allowed to stabilize at a tension of 2 g for 40 min. During that period, the Krebs solution was replaced in 10 min intervals. After that, each tissue bath was filled with 5 mL of the Krebs solution, and the tension was set at 1 g (basal tension). The viability of the aortic rings was verified through the contraction mediated by noradrenaline (1 μM), followed by the addition of acetylcholine (100 μM).
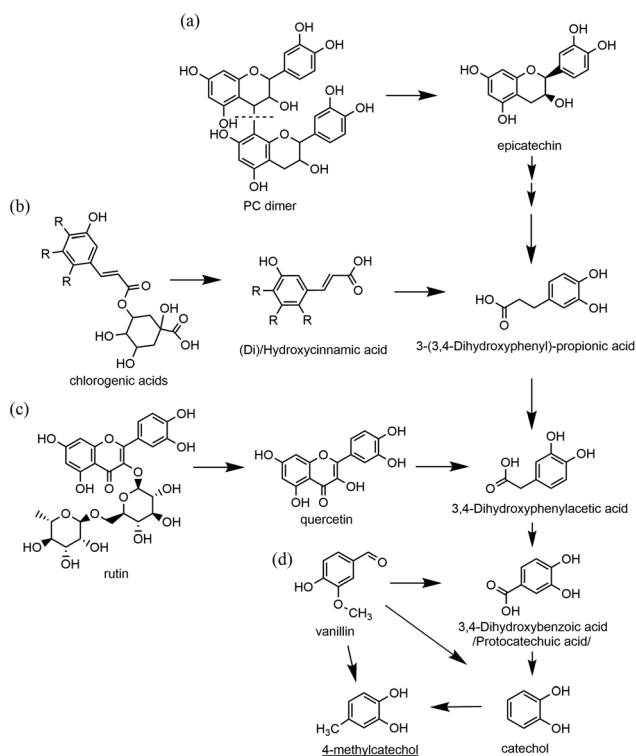
Mechanistic experiments. Taking into account prior experiments suggesting that 4-MC-induced vasorelaxation is independent of endothelium integrity,[14] the current mechanistic study using different activators/inhibitors (Table 1) was executed on endothelium-denuded aortic rings. To test the influence of activators of cyclic nucleotide synthesis on relaxation, noradrenaline-precontracted aortic rings were treated with 4-MC (at 15 μM, *i.e.*, a concentration able to cause ∼15–20% of the maximal relaxation), followed by the cumulative addition of the NO donor, SNP (100 pM–1 μM), or the adenylyl cyclase activator, forskolin (100 pM–1 μM). To explore the possible involvement of soluble guanylate cyclase (sGC), its inhibitor ODQ (1 μM) was applied for 30 min, followed by the contraction with noradrenaline and cumulative addition of 4-MC (100 nM–100 μM). The role of protein kinase G (PKG) was investigated by treating the aortic rings with inhibitors of PKG: DT3 (1 μM) or Rp-8-pCPT-cGMPS (1 μM) for 30 min before the contraction induced by noradrenaline (10 μM), followed by the addition of 4-MC at a concentration causing ∼80% of the maximal relaxation. In other experiments, the aortic rings were pre-treated with various K^+ channel inhibitors, namely, iberiotoxin (20 nM), glibenclamide (10 μM), $BaCl_2$ (50 μM), 4-aminopyridine (3 mM), or linopirdine (10 μM) for 30 min, followed by the addition of noradrenaline. Once the contraction reached the plateau, 4-MC was cumulatively added (100 nM–100 μM). As the negative control, the rings were pre-treated with the vehicle of the respective inhibitor, instead of the latter. To explore the role of L-type calcium channels ($Ca_V1.2$), the aortic rings were pre-treated with 15 mM KCl, followed by incubation with 4-MC for 30 min, at concentrations causing 20% and 80% of the maximal relaxation. Then, a L-type calcium channel activator, Bay K8644, was added cumulatively (100 pM–1 μM) in the dark to induce a contractile response. KCl (60 mM) was used to induce maximal contraction. As the

negative control, the same concentration of DMSO without the tested compound was applied in the incubation step. Nifedipine (150 nM), a standard L-type calcium channel inhibitor, was used as the positive control.

Lastly, the aortic rings were treated with the sarco/endoplasmic reticulum calcium ATPase (SERCA) inhibitor thapsigargin (1 μM), followed by the addition of noradrenaline (10 μM) in the presence of 7 mM KCl. Once the contraction was stable, 4-MC was applied at a concentration causing ∼80% of the maximal relaxation. As the negative control, the rings were treated with the vehicle of the respective inhibitor in the incubation step.

Measurement of cAMP

Smooth muscle cell line. The A10 rat embryonic thoracic aorta smooth muscle cell line was obtained from American Type Culture Collection. Cells were cultivated in Advanced DMEM/F12 medium (Gibco, #12634028) supplemented with 10% of foetal bovine serum (Gibco, #10500064), 1% HEPES, and 1% penicillin/streptomycin solution at 37 °C in a humidified atmosphere of 5% CO_2 in air. The culture was passaged twice weekly once they reached approx. 80% confluence. After passage, cells were seeded into 12-well plate with a seeding density of 100 000 cells per well, and left to grow for 2 days to reach full confluency. Cells were treated with 10 μL of inducer with or without 4-MC (both dissolved in DMSO) mixed with 390 μL of the media for 1 minute, and the reaction was stopped by the addition of 400 μL of 1% Triton X-100 in 0.1 M HCl. The suspension was incubated for 10 minutes in a 37 °C ultrasonic bath, and spun down for 2 min at 10 500 g. The supernatant was stored at −80 °C until the cAMP was determined.

Human platelets. All healthy volunteers had given written informed consent for the study. The study was approved (No. UKFaF/176666/2021-2), and performed under the supervision of the Ethics Committee of Charles University, Faculty of Pharmacy in Hradec Králové. It conformed to the latest Declaration of Helsinki. Blood was collected in EDTA test tubes and centrifuged at 214g for 8 minutes by VWR Compact Star CS4 (VWR International Ltd, U.K.). The obtained supernatant (platelet rich plasma) was again centrifuged at 2000g for 1 minutes. The supernatant was discharged, and the pellet was resuspended in Krebs solution without calcium. The number of platelets was calculated in the Neubauer chamber and adjusted to 0.5×10^8 platelets per ml. This platelet suspension (390 μL) was treated with inducers with or without 4-MC (both dissolved in DMSO, total volume 10 μL) precisely for 1 minute. The reaction was stopped by the addition of 1% Triton X-100 in 0.1 M HCl, and left for 10 minutes in an ultrasonic bath. The supernatant was used for cAMP determination after centrifugation at 10 500g.

The level of cAMP was assessed by ELISA (ab290713, Abcam, U.K.), according to the instructions of the manufacturer.

Molecular docking and interaction analysis

Ligand preparation. All ligand structures were retrieved from PubChem[23] in SDF format, followed by energy minimization

Table 1 Target proteins investigated in the mechanistic studies of 4-methylcatechol (4-MC), and activators/inhibitors used in the *in vitro* experiments on the isolated rat aorta

Targets	Activator (A)/ inhibitor (I)
Ion channels	
L-type Ca^{2+} channels ($Ca_V1.2$)	Bay K8644 (A)
	Nifedipine (I)
BK_{Ca} (large conductance calcium- activated K^+ channels)	Iberiotoxin (I)
K_{ATP} (ATP-sensitive K^+ channels)	Glibenclamide (I)
K_{IR} (inwardly-rectifier K^+ channels)	Ba^{2+} (I)
K_V (voltage-gated K^+ channels)	4-Aminopyridine (I)
K_V7 (voltage-gated K^+ channels K_V7 subfamily)	Linopirdine (I)
Enzymes	
sGC (soluble guanylate cyclase)	Sodium nitroprusside (A)
	ODQ (I)
PKG-Iα (protein kinase G isoform Iα)	DT3 (I)
PKG-Iα,β (protein kinase G isoforms Iα,β)	Rp-8-pCPT-cGMPS (I)
AC (adenylate cyclase)	Forskolin (A)
ATPases	
SERCA (sarco/endoplasmic reticulum calcium ATPase)	Thapsigargin (I)

using the MM2 force field feature built in the Chem3D v. 22.0 (PerkinElmer, Waltham, Massachusetts, U.S.A.), and finally converted to PDB format.

Protein preparation. The crystal structures of the target proteins were obtained from the RCSB Protein Data Bank (PDB).[24] Prior to docking analysis, the proteins were prepared using UCSF Chimera built-in Dock Prep v. 1.15 (the Resource for Biocomputing, Visualization, and Informatics at the University of California, San Francisco, U.S.A.). In the preparation of the protein, water molecules were extracted, the missing residues were repaired, hydrogen atoms were added, and partial charges were assigned. The PDB provided 9 target proteins with crystal structures that satisfied the criteria for molecular docking studies (Fig. 2).

Molecular docking analysis. Molecular docking calculations were performed using UCSF Chimera built-in AutoDock Vina tool v. 1.15 (the Resource for Biocomputing, Visualization, and Informatics at the University of California).[25] The grid box and box center were arranged according to each target protein to cover the active binding site and all essential residues. Other parameters were kept at default values. The best-docked poses of 4-MC were selected based on the lowest docking score, followed by the comparison of interactions with those of each reference ligand in the binding cavity of the target proteins. The protein–ligand interactions were determined again using Chimera[26] by displaying residues within 5 Å from the ligand pose and Discovery Studio Visualizer (Discovery Studio 2020 v20.1.0.19295) for 2D interaction.

Data analysis. GraphPad Prism v. 9.2.0 (GraphPad Software, San Diego, CA, USA) was used for data analysis. Concentration–response curves were fitted by nonlinear regression. The significance of the results was assessed through the Student unpaired t-test. In the experiments with Bay K8644, two-way analysis of variance (ANOVA) was used, followed by the Holm-Šidák multiple comparison test. Data are shown as mean ± SEM of at least three independent experiments.
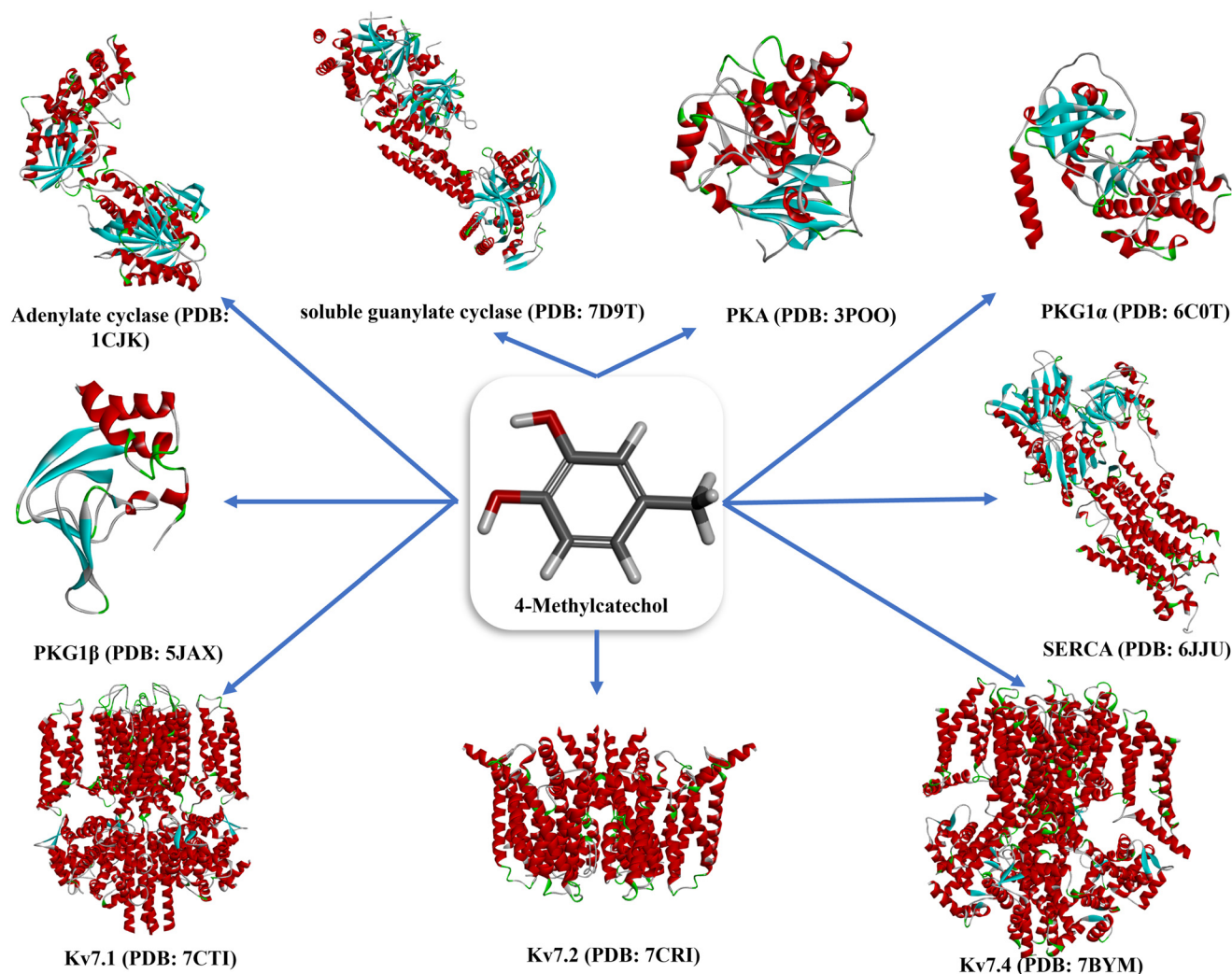

Fig. 2 Structures of 4-methylcatechol and the target proteins used for reverse docking.

Results

Cyclic nucleotide pathways

In the first step, the possible involvement of the cyclic guanosine monophosphate (cGMP) or cyclic adenosine monophosphate (cAMP) pathways in the 4-MC-induced vasorelaxation was investigated. For this reason, SNP, a NO donor that activates soluble guanylyl cyclase (sGC), and forskolin, an activator of adenylate cyclase, were used. In the presence of 4-MC, the

vasodilatory effects of both activators were potentiated (Fig. 3A and B). Due to this fact, the involvement of sGC, which produces cGMP, and PKG, which is a downstream target of cGMP, was analyzed. No significant differences were found after inhibition of sGC with ODQ (Fig. 3C), nor inhibition of different PKG isoforms; Iα by DT3 and Iα,β by Rp-8-pCPT-cGMPS (Fig. 3D). Hence, sGC and PKG are not the targets of 4-MC. To see the possible involvement of the cAMP pathway, the cAMP levels were measured in rat VSMC (ESI Fig. S1†). 4-MC was not
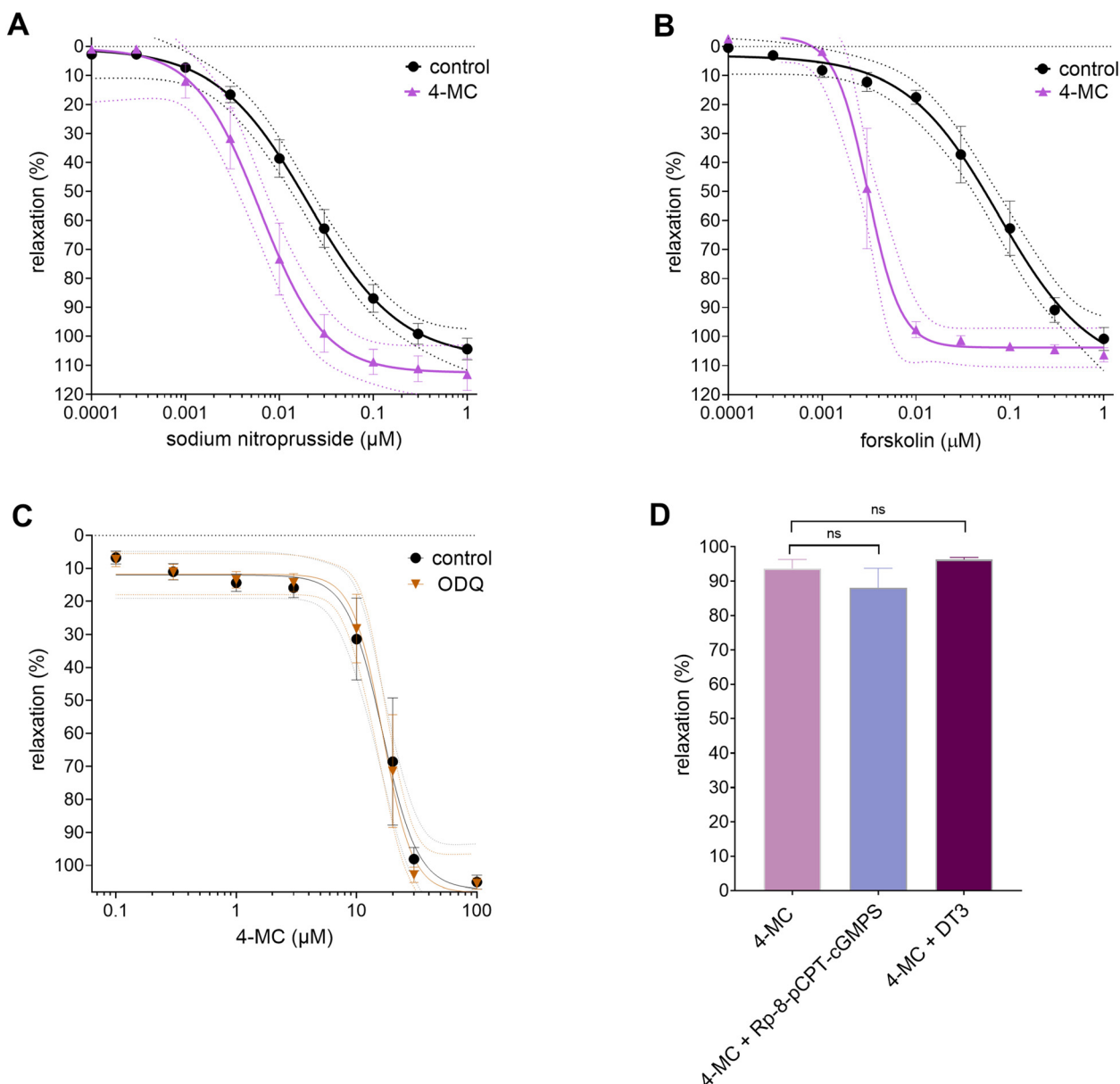

Fig. 3 (A) Effect of 4-methylcatechol (4-MC, 15 μM) on relaxation induced by sodium nitroprusside. (B) Effect of 4-MC (15 μM) on relaxation induced by forskolin. (C) Concentration-dependent curves obtained with 4-MC in the presence and absence of the soluble guanylate cyclase inhibitor ODQ (1 μM). (D) Impact of inhibition of PKG-Iα,β isoforms by Rp-8-pCPT-cGMPS (1 μM) or DT-3 (1 μM) on 4-MC-induced vasorelaxation (70 μM, *i.e.*, concentration able to induce ∼80% relaxation). Controls: (A and B) aortic rings were treated with cumulative concentrations of the activators sodium nitroprusside and forskolin in the absence of the tested compound 4-MC. (C) and (D) Aortic rings were treated with 4-MC in the absence of the inhibitor. Each point represents mean ± SEM from at least five separate experiments, except for (D), where *n* = 4 for each group. ns = not significant.

able to modify the levels of cAMP in these cells, whether alone or in combination with forskolin, prostaglandin E_2 or serotonin. As the cells had relatively high basal cAMP levels and only the combination of forskolin with theophylline (a non-selective inhibitor of phosphodiesterase) was able to markedly increase the cAMP levels, we decided to confirm these results in another model. Human platelets were selected, as they had very low basal levels of cAMP, and responded well to low concentration of forskolin. 4-MC did not modify the basal levels of cAMP in resting platelets, and it had also no impact on the raised levels of cAMP after treatment with forskolin, prostaglandin E_2 or adenosine (ESI Fig. S1†). This suggests that 4-MC cannot activate adenylyl cyclase or block phosphodiesterase, in contrast to a clear impact of the non-selective phosphodiesterase inhibitor theophylline.

As cyclic nucleotide pathways are likely not involved, attention was then given to ion channels, which are the other known downstream targets of cyclic nucleotide-mediated vasodilatory pathways.

BK_{Ca}, K_{ATP}, K_{IR} and K_V channels

Potassium channel opening is modulated by intracellular signaling pathways involving cyclic nucleotides (Fig. 4). The opening of vascular K^+ channels leads to hyperpolarization of the VSMCs with consequent vasodilation. No significant differences were found before and after the inhibition of BK_{Ca}, K_{ATP}, or K_{IR} channels with their respective inhibitors, iberiotoxin (Fig. 4A), glibenclamide (Fig. 4B), or Ba^{2+} (Fig. 4C). On the other hand, inhibition of K_V channels by 4-aminopyridine caused about 60% reduction in the maximum relaxation caused by 4-MC (Fig. 4D). Furthermore, selective inhibition of K_V7 channels with linopirdine also caused a significant but lower decrease in the vasodilatory effect, indicating that K_V7 channels are partially involved in the effect of 4-MC (Fig. 4E).

L-type Ca^{2+} channels and SERCA

The excitability and contractility of VSMCs are regulated through the interplay between K^+ and Ca^{2+} channels. L-type Ca^{2+} channels have the opposite role in mediating vasoconstriction due to VSMC depolarization. Therefore, in the next step, we sought to explore whether L-type Ca^{2+} channels were inhibited in the presence of 4-MC. In this case, an L-type Ca^{2+} channel activator, Bay K8644, was cumulatively added to the aortic rings to induce a contractile response. 4-MC did not abolish the Bay K8644-elicited vasoconstriction at any of the tested concentrations, *i.e.*, low and high concentrations (30 and 70 μM), in contrast to the clinically used well-known L-type Ca^{2+} channel blocker nifedipine (Fig. 5A). A higher concentration of 4-MC even potentiated the effect of Bay K8644, rendering the possible inhibitory effect of 4-MC on the L-type Ca^{2+} channel highly improbable. The cytosolic calcium concentrations are also dependent on SERCA. For this reason, we decided to also test the hypothesis that 4-MC activates SERCA, as the observed vasodilation could be due to the decreasing cytosolic calcium. The pretreatment of the norepinephrine-precontracted aortic rings with the inhibitor of SERCA, thapsigar-

gin, caused a significant but not complete decrease in the extent of relaxation induced by 4-MC, showing that this hypothesis might not be simply rejected (Fig. 5B).

Molecular docking and intermolecular interaction

One of the hydroxyl groups on 4-MC undergoes sulfonation in the circulation of plasma. Therefore, docking studies were performed not only on 4-MC, but also on 4-methylcatechol-1-sulfate (4-MC-1-S) and 4-methylcatechol-2-sulfate (4-MC-2-S). The docking scores of 4-MC, 4-MC-1-S and 4-MC-2-S (Table 2 and Table S1†) were lower than all reference ligands of each target protein, but showed higher ligand efficiencies than the reference ligands, particularly in the case of 4-MC. The ligand efficiency is a measurement of the binding energy per non-hydrogen atom of the ligand on the target protein, or simply the free binding energy divided by the number of heavy atoms.[27] Ligand efficiency can be used to determine whether the ligand has an optimal position on the binding site of the protein through the formation of multiple contacts.[27]

Based on the ligand efficiency value, 4-MC (>0.65) showed the potential to interact with PKGIα, PKA, $K_V7.1$, $K_V7.2$, and $K_V7.4$, which meant that they can be possible 4-MC targets (Table 2).

These data agree with most of our experimental results, concluding that sGC, PKGIβ, adenylate cyclase, and possibly SERCA can be excluded from the list of potential targets of 4-MC. Interestingly, in the case of PKGIα and PKA, their ligand efficacy values were higher. However, as in the prior *in vitro* experiments, the inhibitor DT3 did not affect the vasodilatory effects of 4-MC. PKGIα was also ruled out as a potential target, in addition to PKA. On the other hand, our docking results further support the hypothesis that K_V channels, in particular $K_V7.1$, $K_V7.2$, and $K_V7.4$, might be potential targets of 4-MC (Table 2).

Molecular docking approaches allow the modelling of the interactions between ligands and proteins at the atomic level, enabling the characterization of ligand behaviour in the ligand-binding domain to elucidate fundamental biochemical processes.[28] Overall, the docking poses of 4-MC, and its 1- and 2-sulfates are similar to each other, and have analogous interactions with each target protein (Fig. S2–7†). The docking of 4-MC on a binding domain of the protein that overlaps with a reference ligand reflects the higher chances of biologically relevant interactions and biochemical effects.

The best-docked poses of 4-MC on the ligand-binding domains of the abovementioned improbable targets (namely, adenylate cyclase, PKA, sGC, PKGIα, PKGIβ and SERCA) are shown as complementary results in the supplementary data (Fig. S2–S4†). Notably, at this stage of our study, the compilation of the ligand efficiency and the best docked poses confirmed, as initially hypothesized, that K_V channels are involved in the vasodilatory effect of 4-MC. Although the above-reported docking scores suggested that $K_V7.1$ could be the target, the participation of this channel is improbable because the best-docked pose of 4-MC did not overlap with the reference ligand ML277 (Fig. 6A). The molecular interactions between 4-MC or
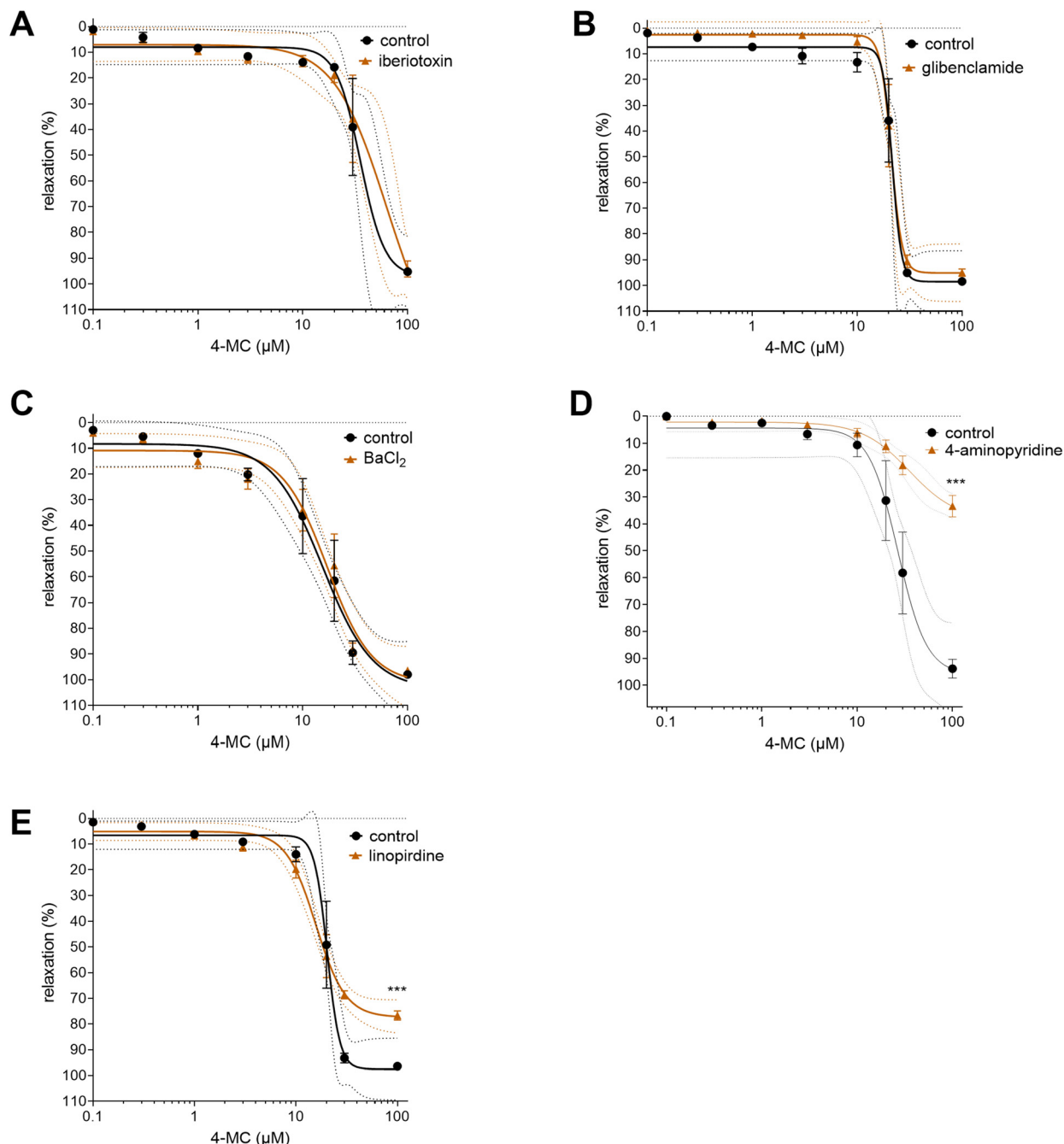
Fig. 4 (A) Effect of inhibition of vascular potassium (K^+) channels (BK_{Ca}, K_{ATP}, K_{IR} and K_V) on the vasodilatory activity of 4-methylcatechol (4-MC). Concentration-dependent curves for the vasorelaxation induced by 4-MC in the absence (controls) and presence of (A) iberiotoxin (20 nM), (B) glibenclamide (10 μM), (C) $BaCl_2$ (50 μM), (D) 4-aminopyridine (3 mM), and (E) linopirdine (10 μM). Each point represents mean $\pm$ SEM from at least five separate experiments. BK_{Ca}, large conductance calcium-activated K^+ channels; K_{ATP}, ATP-sensitive K^+ channels; K_{IR}, inwardly rectifying K^+ channels; K_V, voltage-gated K^+ channels; ***$p < 0.001$ *vs.* control.

the reference ligand at the ligand binding domain of each target protein are summarized in Table S1.† Some residues involved in the interaction between 4-MC and the target protein were the same as in the interaction between the reference ligand and the protein.

In the case of the $K_V7.2$ channel, the best docked pose of 4-MC overlapped with the reference ligand retigabine (Fig. 6B),

and both ligands formed H-bonds with Trp236 (Fig. 7). Moreover, Phe305 and Leu299 were shared residues, albeit with different interactions involved; namely, H-bonds in the case of retigabine, and hydrophobic contacts in the case of 4-MC (Fig. 7). Concerning the $K_V7.4$ channel, besides the observed overlapping docked poses between 4-MC and the reference ligand retigabine (Fig. 6C), similar types of inter-
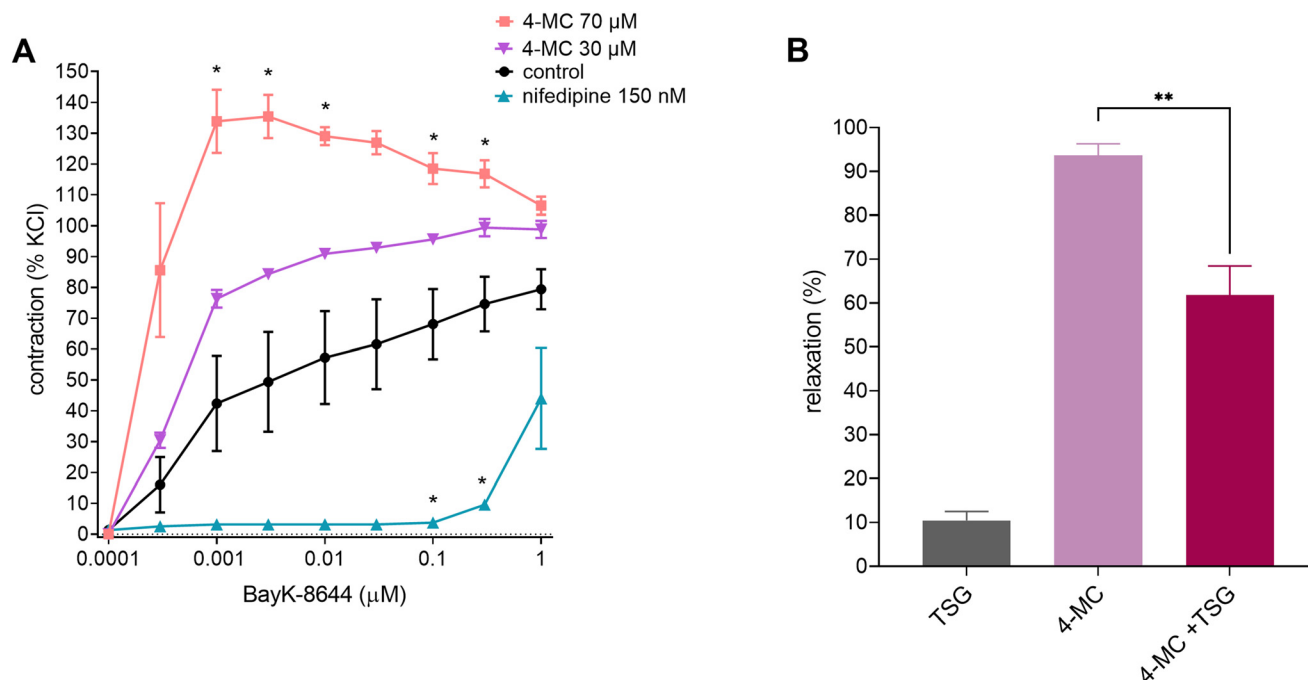
Fig. 5 Effect of 4-methylcatechol (4-MC) on vessel tonus as a function of extracellular (A) and intracellular (B) calcium. (A) Effect of pretreatment of rat aortic rings with 4-MC (70 and 30 μM) on the Bay K8644 (100 pM–1 μM)-elicited contraction of aortic rings. Nifedipine (150 nM) and DMSO were used as the positive and negative controls, respectively. Data were calculated from the maximal contraction induced by KCl (60 mM). *$p < 0.05$ as compared to the negative control using two-way ANOVA, followed by the Holm-Šidák multiple comparison test. (B) Impact of the sarco/endoplasmic reticulum calcium ATPase (SERCA) inhibitor thapsigargin (TSG, 1 μM) on 4-MC (70 μM)-induced vasorelaxation. Vessels were precontracted with norepinephrine (10 μM), and the degree of vasodilation was measured thereafter. As the negative control, the rings were treated with thapsigargin (TSG) and the solvent DMSO. As the positive control, the relaxation-induced 4-MC was measured in the absence of TSG. **$p < 0.01$ as compared to the positive control using Student's unpaired t-test. Each point represents the mean ± SEM from at least five separate experiments, except for (B) n = 4 for control, n = 5 for 4-MC and n = 5 for 4-MC + TSG.

Table 2 Docking scores of 4-methylcatechol (4-MC) for each target protein

PDB ID	Target protein	Docking score (kcal mol^{-1})		Docking score differences
		Reference ligand	4-MC	(Reference ligand) – (4-MC)
7D9T	sGC	−10.7	−5.3	5.4
6C0T	PKGIα	−8.2	−6.5	1.7
5JAX	PKGIβ	−11.6	−6.0	5.6
3POO	PKA	−9.3	−5.9	3.4
7TCI	K$_V$7.1	−8.8	−6.0	2.8
7CR1	K$_V$7.2	−8.1	−6.1	2.0
7BYM	K$_V$7.4	−7.6	−6.0	1.6
1CJK	AC	−9.7	−5.6	4.1
6JJU	SERCA	−9.7	−5.5	4.2

PDB ID, Protein Data Bank Identifiers; sGC, soluble guanylate cyclase; PKGIα, protein kinase G isoform Iα; PKGIβ, protein kinase G isoform Iβ; PKA, protein kinase A; K$_V$, voltage-gated potassium channel; AC, adenylate cyclase; SERCA, sarco/endoplasmic reticulum calcium-ATPase.

actions were found. In some cases, they were formed with shared residues. It is noteworthy that some of the residues involved, namely Trp242 and Phe246, are crucial for the acti-

vation of the K$_V$7.4 channel.[29] The best-docked pose of 4-MC in the K$_V$7.4 binding cavity was stabilized by H-bonds and hydrophobic interactions. H-bonds were formed between the hydroxyl group of 4-MC (Fig. 7) and the amine groups of Ala241 and Phe246, and the carboxyl group of Phe310, amino acids present on the K$_V$7.4 protein backbone. Similarly, H-bonds (Fig. 7) were established between retigabine and specific residues of the K$_V$7.4 protein backbone: (1) an O atom and the Trp242 side chain, (2) an amine group with the Ser309 side chain, and (3) an amine group with the Leu305 and Phe311 carboxyl groups. Interestingly, due to the proximity of the benzyl groups of both ligands to the aromatic side chain of Trp242, the same π–π interaction with Trp242 was found for both 4-MC and retigabine (Fig. 7). Furthermore, retigabine and 4-MC interacted with Phe246, albeit distinctly, through π–π and H-bond interactions (Fig. 7), respectively.

Discussion

In the current study, we set out to elucidate the mechanism of the vasodilatory activity of 4-MC as a follow-up to our previous research.[15] To achieve a more complex picture, both *in vitro* and *in silico* approaches were employed. The obtained results
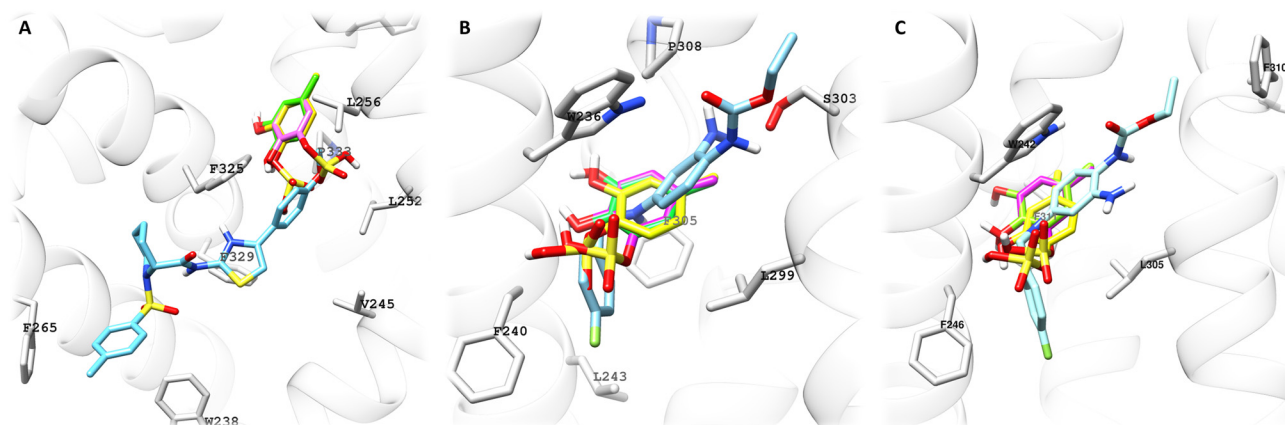
Fig. 6 Docking pose of 4-methylcatechol (green), 4-methylcatechol-1-sulfate (yellow), 4-methylcatechol-2-sulfate (purple), and retigabine (turquoise) in the ligand binding domain of the human voltage-gated potassium channel: (A) $K_V7.1$; (B) $K_V7.2$; (C) $K_V7.4$.
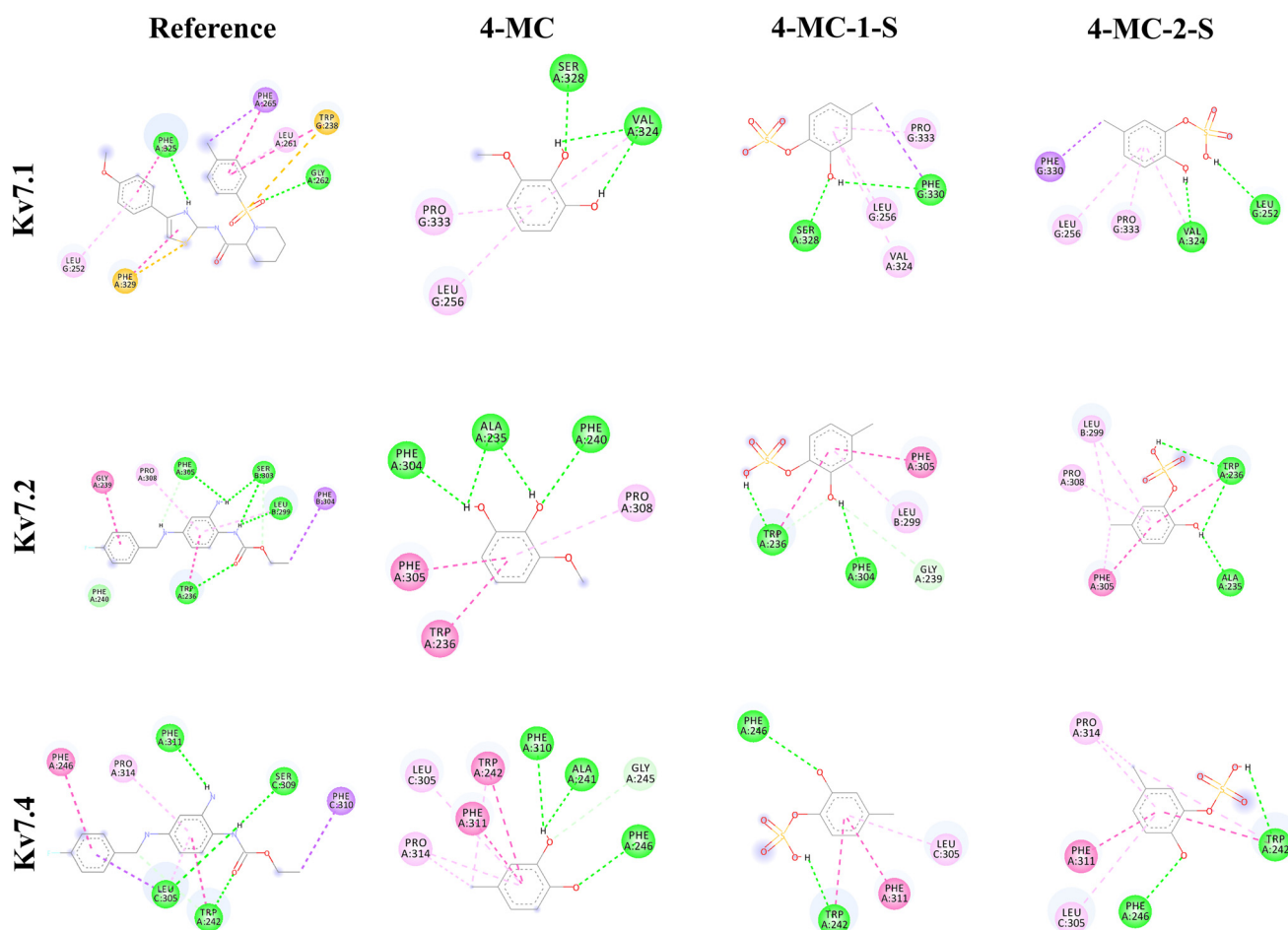

Fig. 7 2D representation of molecular interactions between the reference ligand (ML277 for $K_V7.1$ and retigabine for $K_V7.2$; 7.4), 4-methylcatechol (MC), 4-methylcatechol-1-sulfate (4-MC-1-S), and 4-methylcatechol-2-sulfate (4-MC-2-S). Dashed green lines show the hydrogen bond interactions; dashed purple lines indicate the hydrophobic interactions.

apparently fit together and enabled us to overcome the inherited problems of experiments, *e.g.*, the absence of known and selective activators or inhibitors, and docking, *i.e.*, the need

for experimental confirmation of *in silico* results. In reverse docking, the docking score between the ligand and the target protein serves as an evaluation criterion to rank the potential

targets of the ligand. To accomplish target evaluation, reverse docking analysed whether the ligand could fit into the ligand binding site of the target protein, and evaluated the critical interactions between the ligand and protein. These two factors were used to determine the potential target of 4-MC.

In the presence of 4-MC, a potentiation of the vasodilation of the rat aorta mediated by cGMP- and cAMP-pathways was observed. As the hypothesis of direct activation of sGC/PKG or impact on cAMP was subsequently ruled out, we concentrated on other downstream targets of cyclic nucleotide pathways, particularly ion channels, which are known to be involved in vasodilation/constriction of arteries. Interference with calcium influx through L-type Ca^{2+} channels can be excluded, but the involvement of potassium (K_V) channels and specifically the K_V7 subtype was observed.

Nevertheless, the mechanism of 4-MC-induced vasorelaxation is not solely based on the activation of K_V7 channels. Moreover, inhibition of all K_V channels by 4-AP did not fully abolish the vasodilatory effect of 4-MC (Fig. 4D). Besides that, the extent to which the selective inhibitor of K_V7 channels, linopirdine, lessened the maximum vasodilatory effect of 4-MC was much lower than that caused by 4-AP (~15% *vs.* ~60% decrease, Fig. 4E and D), meaning that other subfamilies of K^+ channels could be involved. In fact, the family of K_V channels is highly complex and diverse with 12 subfamilies ($K_V1–K_V12$) in humans.[30] In SMCs, besides the K_V7 channels, K_V1, K_V2, and K_V4 channels are also expressed.[3,31] Moreover, the distribution of each subtype depends on the species and the vascular bed. To obtain a framework, $K_V1.2$, $K_V1.5$, $K_V2.1$, $K_V7.1$, $K_V7.4$, and $K_V7.5$ were identified in blood vessels from rodents, rabbits, dogs, and humans.[32] The role of vascular K_V7 channels should neither be underestimated nor overestimated. This channel family provides roughly 20% of cell ion currents (at −40 mV),[33] and participates in the regulation of the resting membrane potential and the negative feedback of myogenic and vasoconstrictor-induced tone. Among the K_V7 channel subtypes, $K_V7.4$ together with $K_V7.5$ likely play major roles.[34–36] The $K_V7.4$ channel family can be influenced by several vasoactive stimuli (*e.g.*, activation of the cAMP/PKA pathway,[37] cGMP/PKG pathway[38]) in several vascular beds like the renal VSMCs,[37] coronary[39] and cerebral arteries.[40] During vasoconstriction, the activated protein kinase C was reported to inhibit the K_V7 channels.[41] Thus, the K_V7 channels plays an important role in vascular physiology. Nevertheless, it should be kept in mind that the regulation of vascular tone is very complex and involves the interplay of numerous factors.

Complete experimental testing is currently not possible due to the lack of specific activators or inhibitors. Hence, we cannot exclude the fact that other K_V channel subfamilies, not involved in this study, might also be involved. Regardless, our docking study suggested the involvement of the $K_V7.2$ and 7.4 channels. There are additional drawbacks of experimental functional studies with activators/inhibitors, as they cannot provide direct insight into the type of 4-MC interaction with K_V channels, *i.e.*, direct or indirect. Such limitation can be resolved by supplementation with *in silico* data. Indeed, our

in silico data showed that 4-MC could directly bind to K_V channels, further supporting our hypothesis. Concerning $K_V7.2$, H-bonds formed with the residues Phe305 and Ser303 are considered relevant for the stabilization of retigabine.[42] However, the results showed that 4-MC forms hydrophobic interactions with Phe305 (Fig. 7). Moreover, $K_V7.2$ channels are mostly expressed in the central nervous system, where together with $K_V7.3$, they form the "M channel".[43] On the other hand, $K_V7.4$ channels are expressed in the mammalian vasculature,[44] and their involvement was most obvious and strongly supported by the following observations: (a) a very low difference in docking scores (−1.6 kcal mol^{-1}) (Table 2), (b) the best-docked pose for 4-MC that overlapped with that of the reference ligand retigabine (Fig. 7), and (c) the intermolecular interaction analysis demonstrated that crucial residues for $K_V7.4$ activation are involved (Fig. 7).

K_V channels are major determinants of the membrane potential in VSMCs, and are thus essential for the regulation of the vascular tone. Studies have reported on alterations in the function of these channels in cardiovascular diseases. Particularly, a decrease in $K_V7.4$ protein levels was reported in animal models of hypertension.[45]

Although scarce, bioavailability studies reported on human plasma maximum concentrations for the sulphated form of 4-MC ranging from ~2 to 3.5 μM, which were attained within 6 h to 7 h after the ingestion of a mixed berry fruit purée (blueberry, blackberry, raspberry, strawberry tree fruit, and Portuguese crowberry) or cranberry juice.[9,46] 4-MC sulphate was also identified in human plasma after the consumption of natural and enriched apple juices.[16] Therefore, relatively high plasma concentrations of 4-MC can be reached after the ingestion of foods rich in polyphenols. Thus, by targeting $K_V7.4$ channels, 4-MC could likely contribute to the prevention of smooth muscle remodeling. Moreover, it is noteworthy that even before the consumption of the purée, this conjugate was already present in plasma from the volunteers, albeit at lower levels, *i.e.*, ~300 nM.[46]

The docking study also allows us to answer the question of whether SERCA is involved. Experimental testing showed that inhibition of SERCA by thapsigargin decreased the vasodilation caused by 4-MC (Fig. 5B). This suggested that SERCA could be a possible target. Such experimental data could not bring a clear answer, as there is a tight interplay of K^+ and Ca^{2+} currents in modulating the VSMC contractility. The docking study does not confirm 4-MC interaction with SERCA, so the likely explanation is that an elevation in intracellular Ca^{2+} decreased the vasoactive effect of 4-MC mediated by K^+ channels.

Nevertheless, the intriguing nature of the mechanism of 4-MC is evidenced by the fact that with increasing concentrations of 4-MC, a potentiation of the vasocontractile response induced by Bay K8644 was observed (Fig. 5A). The meaning of these findings remains to be clarified. At first sight, it seems a paradox since with increasing cytosolic Ca^{2+} concentrations, VSMCs become depolarized, thereby promoting the activation of K_V channels. It is possible that 4-MC can somehow affect the effect of Bay K8644, which is also dependent on other

conditions.[47,48] Interestingly, others have reported that the parent compound, quercetin, reduces the efficacy of Bay K8644.[49] Under specific conditions favouring the depolarisation of rat arteriae, both quercetin and Bay K8644 potentiated the response to calcium.[50] Nevertheless, it should be also mentioned that 4-MC has a different mechanism at least in other cells, as we recently showed that its antiplatelet potential is based on interference with cyclooxygenase–thromboxane synthase coupling.[51] Notably, the diverse mechanisms of action of 4-MC are reflected in pleiotropic effects that include vasodilatory and antiplatelet activities. In addition, it is important to emphasize the significance of exploring the metabolic pathways, metabolites formed, as well as their pharmacokinetics to better understand the beneficial effects of a diet rich in polyphenols. Under physiological conditions, 4-MC and other metabolites are formed, and may exert synergistic effects. In addition, the existence of large interindividual variability in the microbiota catabolic output[16,52] presents a challenge for further study.

Conclusions

In summary, our findings suggest that the dietary polyphenol metabolite, 4-MC, relaxes the rat aorta through the opening of K_V channels, with partial involvement of the K_V7 subfamily. *In silico* molecular docking studies corroborated the *in vitro* results, and deepened our study at the molecular level. The results showed the overlapping best-docked poses of 4-MC and that of retigabine (the reference ligand) at $K_V7.4$, as well as similar interactions with crucial residues, namely Trp242 and Phe246. However, the existence of other mechanisms apparently contributing to the relaxation of the vasculature by 4-MC is unambiguous. Given the reported pleiotropic effects of 4-MC on the cardiovascular system, further research on this metabolite and its sulfate conjugates is warranted.

Author contributions

Patrícia Dias: writing – original draft, investigation & methodology, data curation, writing – review & editing; Rudy Salam: writing – original draft, investigation & methodology, data curation, writing – review & editing; Jana Pourová: supervision, investigation & methodology, writing – review & editing; Marie Vopršalová: investigation & validation; Lukáš Konečný and Eduard Jirkovský: investigation & methodology, data curation, writing – review & editing; Jurjen Duintjer Tebbens: data curation and formal analysis, supervision; Přemysl Mladěnka: supervision, writing – original draft, review & editing, critical revision of the obtained findings and manuscript content and funding acquisition.

Data availability

The data for this article, including a description, are available at **https://zenodo.org/records/13739740**. There are supplementary data available for this paper (**https://www.rsc.org/supp-data/d3/fo/d3fo04672a/d3fo04672a1.pdf**) as well as research data.

Conflicts of interest

There are no conflicts to declare.

Acknowledgements

References

1 K. T. Mills, A. Stefanescu and J. He, The global epidemiology of hypertension, *Nat. Rev. Nephrol.*, 2020, **16**, 223–237.

2 B. K. Joseph, K. M. Thakali, C. L. Moore and S. W. Rhee, Ion channel remodeling in vascular smooth muscle during hypertension: Implications for novel therapeutic approaches, *Pharmacol. Res.*, 2013, **70**, 126–138.

3 T. A. Jepps, Unravelling the complexities of vascular smooth muscle ion channels: Fine tuning of activity by ancillary subunits, *Pharmacol. Ther.*, 2017, **178**, 57–66.

4 E. A. Pereira da Silva, M. Martín-Aragón Baudel, M. F. Navedo and M. Nieves-Cintrón, Ion channel molecular complexes in vascular smooth muscle, *Front. Physiol.*, 2022, **13**, 999369.

5 P. Mladenka, L. Zatloukalová, T. Filipský and R. Hrdina, Cardiovascular effects of flavonoids are not caused only by direct antioxidant activity, *Free Radicals Biol. Med.*, 2010, **49**, 963–975.

6 C. Del Bo, S. Bernardi, M. Marino, M. Porrini, M. Tucci, S. Guglielmetti, A. Cherubini, B. Carrieri, B. Kirkup, P. Kroon, R. Zamora-Ros, N. H. Liberona, C. Andres-Lacueva and P. Riso, Systematic Review on Polyphenol Intake and Health Outcomes: Is there Sufficient Evidence to Define a Health-Promoting Polyphenol-Rich Dietary Pattern?, *Nutrients*, 2019, **11**, 1355.

7 S. Ghaffari and N. Roshanravan, The role of nutraceuticals in prevention and treatment of hypertension: An updated review of the literature, *Food Res. Int.*, 2020, **128**, 108749.

8 H.-H. Xiong, S.-Y. Lin, L.-L. Chen, K.-H. Ouyang and W.-J. Wang, The Interaction between Flavonoids and Intestinal Microbes: A Review, *Foods*, 2023, **12**, 320.

9 R. P. Feliciano, A. Boeres, L. Massacessi, G. Istas, M. R. Ventura, C. Nunes dos Santos, C. Heiss and A. Rodriguez-Mateos, Identification and quantification of novel cranberry-derived plasma and urinary (poly)phenols, *Arch. Biochem. Biophys.*, 2016, **599**, 31–41.

10 X. Feng, Y. Li, M. Brobbey Oppong and F. Qiu, Insights into the intestinal bacterial metabolism of flavonoids and the

bioactivities of their microbe-derived ring cleavage metabolites, *Drug Metab. Rev.*, 2018, **50**, 343–356.

11 C. Vetrani, A. A. Rivellese, G. Annuzzi, I. Mattila, E. Meudec, T. Hyötyläinen, M. Orešič and A.-M. Aura, Phenolic metabolites as compliance biomarker for polyphenol intake in a randomized controlled human intervention, *Food Res. Int.*, 2014, **63**, 233–238.

12 P. Dias, J. Pourová, M. Vopršalová, I. Nejmanová and P. Mladěnka, 3-Hydroxyphenylacetic Acid: A Blood Pressure-Reducing Flavonoid Metabolite, *Nutrients*, 2022, **14**, 328.

13 I. Najmanová, J. Pourová and P. Mladěnka, A Mixture of Phenolic Metabolites of Quercetin Can Decrease Elevated Blood Pressure of Spontaneously Hypertensive Rats Even in Low Doses, *Nutrients*, 2020, **12**, 213.

14 J. Pourova, I. Najmanova, M. Voprsalova, T. Migkos, V. Pilarova, L. Applova, L. Novakova and P. Mladenka, Two flavonoid metabolites, 3,4-dihydroxyphenylacetic acid and 4-methylcatechol, relax arteries ex vivo and decrease blood pressure in vivo, *Vasc. Pharmacol.*, 2018, **111**, 36–43.

15 I. Najmanová, J. Pourová, M. Vopršalová, V. Pilařová, V. Semecký, L. Nováková and P. Mladěnka, Flavonoid metabolite 3-(3-hydroxyphenyl)propionic acid formed by human microflora decreases arterial blood pressure in rats, *Mol. Nutr. Food Res.*, 2016, **60**, 981–991.

16 K. Trošt, M. M. Ulaszewska, J. Stanstrup, D. Albanese, C. De Filippo, K. M. Tuohy, F. Natella, C. Scaccini and F. Mattivi, Host: Microbiome co-metabolic processing of dietary polyphenols – An acute, single blinded, cross-over study with different doses of apple polyphenols in healthy subjects, *Food Res. Int.*, 2018, **112**, 108–128.

17 L. P. Strand and R. R. Scheline, The Metabolism of Vanillin and Isovanillin in the Rat, *Xenobiotica*, 1975, **5**, 49–63.

18 M. M. Appeldoorn, J.-P. Vincken, A.-M. Aura, P. C. H. Hollman and H. Gruppen, Procyanidin Dimers Are Metabolized by Human Microbiota with 2-(3,4-Dihydroxyphenyl)acetic Acid and 5-(3,4-Dihydroxyphenyl)-γ-valerolactone as the Major Metabolites, *J. Agric. Food Chem.*, 2009, **57**, 1084–1092.

19 M. R. Olthof, P. C. Hollman, M. N. Buijsman, J. M. van Amelsvoort and M. B. Katan, Chlorogenic acid, quercetin-3-rutinoside and black tea phenols are extensively metabolized in humans, *J. Nutr.*, 2003, **133**, 1806–1814.

20 A. Serra, A. Macià, M.-P. Romero, J. Reguant, N. Ortega and M.-J. Motilva, Metabolic pathways of the colonic metabolism of flavonoids (flavonols, flavones and flavanones) and phenolic acids, *Food Chem.*, 2012, **130**, 383–393.

21 A. Serra, A. Macià, M.-P. Romero, N. Anglés, J.-R. Morelló and M.-J. Motilva, Metabolic pathways of the colonic metabolism of procyanidins (monomers and dimers) and alkaloids, *Food Chem.*, 2011, **126**, 1127–1137.

22 M. M. Ulaszewska, K. Trost, J. Stanstrup, K. M. Tuohy, P. Franceschi, M. F.-F. Chong, T. George, A. M. Minihane, J. A. Lovegrove and F. Mattivi, Urinary metabolomic profiling to identify biomarkers of a flavonoid-rich and flavonoid-poor fruits and vegetables diet in adults: the FLAVURS trial, *Metabolomics*, 2016, **12**, 32.

23 S. Kim, J. Chen, T. Cheng, A. Gindulyte, J. He, S. He, Q. Li, B. A. Shoemaker, P. A. Thiessen, B. Yu, L. Zaslavsky, J. Zhang and E. E. Bolton, PubChem in 2021: new data content and improved web interfaces, *Nucleic Acids Res.*, 2020, **49**, D1388–D1395.

24 S. K. Burley, C. Bhikadiya, C. Bi, S. Bittrich, L. Chen, G. V. Crichlow, C. H. Christie, K. Dalenberg, L. Di Costanzo, J. M. Duarte, S. Dutta, Z. Feng, S. Ganesan, D. S. Goodsell, S. Ghosh, R. K. Green, V. Guranović, D. Guzenko, B. P. Hudson, C. L. Lawson, Y. Liang, R. Lowe, H. Namkoong, E. Peisach, I. Persikova, C. Randle, A. Rose, Y. Rose, A. Sali, J. Segura, M. Sekharan, C. Shao, Y. P. Tao, M. Voigt, J. D. Westbrook, J. Y. Young, C. Zardecki and M. Zhuravleva, RCSB Protein Data Bank: powerful new tools for exploring 3D structures of biological macromolecules for basic and applied research and education in fundamental biology, biomedicine, biotechnology, bioengineering and energy sciences, *Nucleic Acids Res.*, 2021, **49**, D437–D451.

25 O. Trott and A. J. Olson, AutoDock Vina: improving the speed and accuracy of docking with a new scoring function, efficient optimization, and multithreading, *J. Comput. Chem.*, 2010, **31**, 455–461.

26 E. F. Pettersen, T. D. Goddard, C. C. Huang, G. S. Couch, D. M. Greenblatt, E. C. Meng and T. E. Ferrin, UCSF Chimera—A visualization system for exploratory research and analysis, *J. Comput. Chem.*, 2004, **25**, 1605–1612.

27 C. H. Reynolds, S. D. Bembenek and B. A. Tounge, The role of molecular size in ligand efficiency, *Bioorg. Med. Chem. Lett.*, 2007, **17**, 4258–4261.

28 B. J. McConkey, V. Sobolev and M. Edelman, The performance of current methods in ligand-protein docking, *Curr. Sci.*, 2002, **83**, 845–856.

29 T. Li, K. Wu, Z. Yue, Y. Wang, F. Zhang and H. Shen, Structural Basis for the Modulation of Human KCNQ4 by Small-Molecule Drugs, *Mol. Cell*, 2021, **81**, 25–37.e4.

30 S. P. Alexander, J. Striessnig, E. Kelly, N. V. Marrion, J. A. Peters, E. Faccenda, S. D. Harding, A. J. Pawson, J. L. Sharman, C. Southan, J. A. Davies and C. Collaborators, THE CONCISE GUIDE TO PHARMACOLOGY 2017/18: Voltage-gated ion channels, *Br. J. Pharmacol.*, 2017, **174**, S160–S194.

31 N. R. Tykocki, E. M. Boerman and W. F. Jackson, Smooth Muscle Ion Channels and Regulation of Vascular Tone in Resistance Arteries and Arterioles, *Compr. Physiol.*, 2017, **7**, 485–581.

32 J. B. Stott, T. A. Jepps and I. A. Greenwood, KV7 potassium channels: a new therapeutic target in smooth muscle disorders, *Drug Discovery Today*, 2014, **19**, 413–424.

33 R. H. Cox and S. Fromme, Functional Expression Profile of Voltage-Gated K(+) Channel Subunits in Rat Small Mesenteric Arteries, *Cell Biochem. Biophys.*, 2016, **74**, 263–276.

34 I. A. Greenwood and S. Ohya, New tricks for old dogs: KCNQ expression and role in smooth muscle, *Br. J. Pharmacol.*, 2009, **156**, 1196–1203.

35 T. A. Jepps, S. P. Olesen and I. A. Greenwood, One man's side effect is another man's therapeutic opportunity: targeting Kv7 channels in smooth muscle disorders, *Br. J. Pharmacol.*, 2013, **168**, 19–27.

36 W. F. Jackson, K(V) channels and the regulation of vascular smooth muscle tone, *Microcirculation*, 2018, **25**, DOI: **10.1111/micc.12421**.

37 P. S. Chadha, F. Zunke, H. L. Zhu, A. J. Davis, T. A. Jepps, S. P. Olesen, W. C. Cole, J. D. Moffatt and I. A. Greenwood, Reduced KCNQ4-encoded voltage-dependent potassium channel activity underlies impaired β-adrenoceptor-mediated relaxation of renal arteries in hypertension, *Hypertension*, 2012, **59**, 877–884.

38 J. B. Stott, V. Barrese, T. A. Jepps, E. V. Leighton and I. A. Greenwood, Contribution of Kv7 channels to natriuretic peptide mediated vasodilation in normal and hypertensive rats, *Hypertension*, 2015, **65**, 676–682.

39 S. Khanamiri, E. Soltysinska, T. A. Jepps, B. H. Bentzen, P. S. Chadha, N. Schmitt, I. A. Greenwood and S. P. Olesen, Contribution of Kv7 channels to basal coronary flow and active response to ischemia, *Hypertension*, 2013, **62**, 1090–1097.

40 P. S. Chadha, T. A. Jepps, G. Carr, J. B. Stott, H. L. Zhu, W. C. Cole and I. A. Greenwood, Contribution of kv7.4/kv7.5 heteromers to intrinsic and calcitonin gene-related peptide-induced cerebral reactivity, *Arterioscler., Thromb., Vasc. Biol.*, 2014, **34**, 887–893.

41 A. R. Mackie, L. I. Brueggemann, K. K. Henderson, A. J. Shiels, L. L. Cribbs, K. E. Scrogin and K. L. Byron, Vascular KCNQ potassium channels as novel targets for the control of mesenteric artery constriction by vasopressin, based on studies in single cells, pressurized arteries, and in vivo measurements of mesenteric vascular resistance, *J. Pharmacol. Exp. Ther.*, 2008, **325**, 475–483.

42 X. Li, Q. Zhang, P. Guo, J. Fu, L. Mei, D. Lv, J. Wang, D. Lai, S. Ye, H. Yang and J. Guo, Molecular basis for ligand activation of the human KCNQ2 channel, *Cell Res.*, 2021, **31**, 52–61.

43 D. A. Brown and G. M. Passmore, Neural KCNQ (Kv7) channels, *Br. J. Pharmacol.*, 2009, **156**, 1185–1195.

44 A. L. Fosmo and Ø. B. Skraastad, The Kv7 Channel and Cardiovascular Risk Factors, *Front. Cardiovasc. Med.*, 2017, **4**, 75.

45 T. A. Jepps, P. S. Chadha, A. J. Davis, M. I. Harhun, G. W. Cockerill, S. P. Olesen, R. S. Hansen and I. A. Greenwood, Downregulation of Kv7.4 channel activity in primary and secondary hypertension, *Circulation*, 2011, **124**, 602–611.

46 R. C. Pimpão, M. R. Ventura, R. B. Ferreira, G. Williamson and C. N. Santos, Phenolic sulfates as new and highly abundant metabolites in human plasma after ingestion of a mixed berry fruit purée, *Br. J. Nutr.*, 2015, **113**, 454–463.

47 G. Thomas, M. Chung and C. J. Cohen, A dihydropyridine (Bay k 8644) that enhances calcium currents in guinea pig and calf myocardial cells. A new type of positive inotropic agent, *Circ. Res.*, 1985, **56**, 87–96.

48 C. Van Hove, C. Van der Donckt, A. Herman, H. Bult and P. Fransen, Vasodilator efficacy of nitric oxide depends on mechanisms of intracellular calcium mobilization in mouse aortic smooth muscle cells, *Br. J. Pharmacol.*, 2009, **158**, 920–930.

49 S. Saponara, G. Sgaragli and F. Fusi, Quercetin antagonism of Bay K 8644 effects on rat tail artery L-type Ca(2+) channels, *Eur. J. Pharmacol.*, 2008, **598**, 75–80.

50 A. Trezza, O. Spiga, P. Mugnai, S. Saponara, G. Sgaragli and F. Fusi, Functional, electrophysiology, and molecular dynamics analysis of quercetin-induced contraction of rat vascular musculature, *Eur. J. Pharmacol.*, 2022, **918**, 174778.

51 M. Hrubša, L. Konečný, M. Paclíková, M. S. Parvin, P. Skořepa, F. Musil, J. Karlíčková, L. Javorská, K. Matoušová, L. K. Krčmová, A. Carazo, A. Šmahelová, V. Blaha and P. Mladěnka, The Antiplatelet Effect of 4-Methylcatechol in a Real Population Sample and Determination of the Mechanism of Action, *Nutrients*, 2022, **14**, 4798.

52 G. D. Wu, C. Compher, E. Z. Chen, S. A. Smith, R. D. Shah, K. Bittinger, C. Chehoud, L. G. Albenberg, L. Nessel and E. Gilroy, Comparative metabolomics in vegans and omnivores reveal constraints on diet-dependent gut microbiota metabolite production, *Gut*, 2016, **65**, 63–72.